Role of the Hydrophobic Segment of Diacylglycerol Kinase ϵ[†]

Armela O. Dicu,[‡] Matthew K. Topham,[§] Lindsay Ottaway,[‡] and Richard M. Epand*[,‡]

Department of Biochemistry and Biomedical Sciences, McMaster University Health Science Center, Hamilton, Ontario L8N 3Z5, Canada, and Huntsman Cancer Institute, University of Utah, Salt Lake City, Utah 84112

Received November 30, 2006; Revised Manuscript Received March 19, 2007

ABSTRACT: Diacylglycerol kinase ϵ (DGKϵ) is unique among mammalian DGK isoforms in having a segment of hydrophobic amino acids. We have evaluated the contributions of this segment to the membrane interactions and functions of this protein. To test the role of the hydrophobic segment, we have compared the properties of DGKϵ with those of a truncated form of the protein (DGK$\Delta\epsilon$) lacking the 40 N-terminal amino acids, which includes the hydrophobic segment. The proteins were expressed in COS-7 cells from a gene for human DGKϵ or from a gene for a truncated form (DGK$\Delta\epsilon$), both of which had a FLAG tag at the amino terminus. Full-length FLAG-DGKϵ and truncated FLAG-DGK$\Delta\epsilon$ were both more specific for 1-stearoyl-2-arachidonoyl-*sn*-glycerol than for 1,2-dioleoyl-*sn*-glycerol. 1-Stearoyl-2-linoleoyl-*sn*-glycerol exhibited intermediate specificity for both forms of the enzyme. The results show that the truncated form of the enzyme maintains substrate specificity for lipids with an arachidonoyl moiety present at the *sn*-2 position. The truncation increases the catalytic rate constant for all three substrates and may suggest a role in the negative regulation of this enzyme. A full-length DGKϵ with a C-terminal His tag exhibited substrate specificity similar to that of the other two forms of the enzyme, indicating that the nature and position of the epitope tag did not strongly affect this property. Using an ultracentrifugation floatation assay, we showed that at neutral pH DGK$\Delta\epsilon$ is extracted with 1.5 M KCl while DGKϵ remains essentially fully membrane bound. The full-length protein had a weak tendency to oligomerize in the presence of weak detergents. DGKϵ was monomeric on SDS−PAGE but exhibited partial dimerization with low concentrations of perfluorooctanoic acid. The major conclusions of this work are that the hydrophobic domain of DGKϵ does not contribute to substrate specificity but plays a role in permanently sequestering the enzyme to a membrane.

DGKs[1] influence many signaling pathways because both the substrate (DAG) and the product (PA) of these kinases have signaling properties. The major route for the down-regulation of DAG is its phosphorylation to PA catalyzed by DGK (*1*). In most tissues, the immediate response to receptor activation is PtdIns(4,5)P2 hydrolysis, followed rapidly by an increased rate of turnover of PtdIns and PtdInsP to maintain PtdIns(4,5)P2 levels (*2*). The receptor-mediated hydrolysis of PtdIns(4,5)P2 by the PtdIns(4,5)P2-specific PLC mediates one of the intracellular signal transduction pathways in eukaryotic cells and gives rise to the secondary messengers, DAG and IP3, that are involved in a variety of signaling cascades such as cell growth, differentiation, hormonal and neurotransmitter action, and sensory perception (*3*). In the particular case of the DGK isoform studied in this work, i.e., DGKϵ, its importance in neuronal function has been demonstrated in studies with knockout animals (*4*−*6*). It appears to be true that the physiologically relevant DAGs are the polyunsaturated 1,2-diacyl-*sn*-glycerols derived from PtdIns(4,5)P2 hydrolysis by PtdIns(4,5)P2-specific PLC. This DAG is highly enriched in arachidonic acid because it is formed from PtdIns(4,5)P2 that is also arachidonoyl-rich (*7*, *8*). Only one isoform of DGK, DGKϵ, has specificity for DAG containing arachidonoyl chains (*9*, *10*) as well as other polyunsaturated acyl chains (*11*). Thus, DGKϵ may be responsible for downregulating the DAG signal resulting from inositol cycling.

Phosphatidylinositide-derived DAG binds and activates several signaling proteins such as protein kinase C (PKC), the family of four RasGRP nucleotide exchange factors (*12*), recruits the β2-chimaerins-RasGTPase-activating proteins to membrane compartments, and can activate some ion channels, i.e., transient receptor potential family calcium channels (*13*, *14*). The domains for DAG binding were initially discovered in PKC and called C1 domains. They contain zinc-finger-like repeats with a conserved pattern of Cys and

[†] This work was supported by Canadian Natural Sciences and Engineering Research Council Grant 9848.

* To whom correspondence should be addressed: Department of Biochemistry and Biomedical Sciences, McMaster University Health Science Center, Hamilton, ON L8N 3Z5, Canada. Fax: (905) 521-1397. Telephone: (905) 525-9140, ext. 22073. E-mail: epand@mcmaster.ca.

[‡] McMaster University Health Science Center.

[§] University of Utah.

[1] Abbreviations: DGK, diacylglycerol kinase; DGKϵ, ϵ isoform of DGK; DGK$\Delta\epsilon$, truncated form of DGKϵ lacking a segment of 40 amino acids at the N-terminus; FLAG, N-terminal FLAG epitope tag; His, C-terminal His tag; BAP, bacterial alkaline phosphatase; DAG, diacylglycerol; PA, phosphatidic acid; IP_3, inositol 1,4,5-trisphosphate; PKC, protein kinase C; TM, transmembrane; DOG, 1,2-dioleoyl-*sn*-glycerol; SAG, 1-stearoyl-2-arachidonoyl-*sn*-glycerol; SLG, 1-stearoyl-2-linoleoyl-*sn*-glycerol; DTT, dithiothreitol; OG, octyl β-glucoside; PtdIns(4,5)P2, phosphatidylinositol 4,5-bisphosphate; PtdIns, phosphatidylinositol; mTOR, mammalian target to rapamycin; PAGE, polyacrylamide gel electrophoresis; PFO, perfluorooctanoic acid.

10.1021/bi6024726 CCC: $37.00
Published on Web 04/25/2007

His residues (*3*). Recent evidence indicates that alternative DAG binding target proteins such as chimaerins, protein kinase D, RasGRPs, and Munc 13 are involved in DAG second messenger signaling in the cell. These protein targets contain a C1 domain, and they have been shown to bind DAG with high affinity (*15*). Therefore, their implication in intracellular signaling might be as important as the role of PKC (*3*).

The product of the ATP phosphorylation of DAG, the PA, influences some signaling pathways as well. PA can bind and regulate the activity of numerous enzymes, such as phosphatidylinositol 5-kinases (PtdIns-5-kinases), Ras-GAP, PKCζ, PAK1, and protein phosphatase 1 (*13*). PA has potential mitogenic properties, in part due to its capacity to modulate the mammalian mTOR pathway. The mTOR pathway is important for regulating cell growth and tumor growth (*14*). Therefore, indirectly, DGKs may affect a number of biological events such as cell growth, neuronal transmission, and cytoskeleton remodeling.

The DGK family is widespread among species since DGK isoforms have been identified in *Caenorhabditis elegans*, *Drosophila melanogaster*, and *Arabidopsis thaliana*, while to date, no DGKs have been identified in yeast. Bacteria express only one DGK, but this one has no homology to the DGK in higher species. The mammalian DGK family comprises 10 isoforms, nine of which have been identified and studied extensively, while the 10th, DGK*κ*, has been identified recently (*16*). Moreover, the occurrence of alternative splicing was recently detected in five mammalian DGK genes (*β*, *γ*, *δ*, *ζ*, and *η*) (*13*) and probably occurs in other isotypes as well. All mammalian DGK isoforms have a conserved catalytic domain responsible for kinase activity. In addition, all DGKs have at least two cysteine-rich regions that are predicted to bind DAG to localize DGKs where DAG accumulates in the membrane. Most DGKs have other structural domains that likely have regulatory roles and which separate the isoforms into five families (*17*−*20*). The structural diversity and the tissue- and cell-dependent expression patterns are unique for each isoform, suggesting that each member is regulated by a distinct mechanism and performs distinct functions in particular types of cells (*21*).

One distinct class of mammalian DGKs, type III, seems to have no other domains apart from the Cys-rich regions (C1 domains) and the catalytic domain. DGK*ϵ* is the only known type III isoform. DGK*ϵ* is a 64 kDa protein which has a preference for DAG substrates with an arachidonate moiety. This may also account for the enrichment of PtdIns with arachidonate since one path for its synthesis involves phosphorylation of DAG as the first step (*21*). DGK*ϵ* is also unique in being the only DGK isoform with a predicted transmembrane helix, comprising approximately residues 20−40 (*22*).

This study investigates the importance of the putative transmembrane domain for DGK*ϵ* activity and substrate specificity. We designed a truncated form of DGK*ϵ* that lacked amino acid residues 1−40. The objective of this work was to compare the two constructs in terms of their kinetic properties and their integration into a membrane as well as the tendency of the protein to oligomerize.

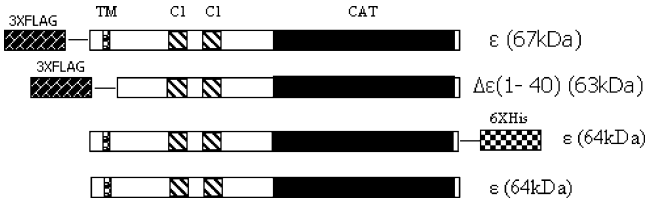

FIGURE 1: DGK*ϵ* constructs used in this study. Diagrams of the three full-length DGK*ϵ* constructs and one truncated DGK*ϵ* mutant are shown. The putative transmembrane domain (TM), the two cysteine-rich domains (C1), and the catalytic domain (CAT) are indicated in the figure, together with the appropriate epitope tag for easier detection and quantification on immunoblots. The C-terminally His-tagged full-length construct has been described in previous studies (*22*). Construction and expression of N-terminally 3XFLAG-tagged full-length and truncated constructs are described in Experimental Procedures. The DGK*ϵ* construct devoid of a tag was designed by M. K. Topham, and the DGK*ϵ* gene was cloned into the pcDNA3 vector from Invitrogen.

EXPERIMENTAL PROCEDURES

*Construction of FLAG Epitope-Tagged DGK*ϵ *Expression Vectors.* A human DGK*ϵ* PCR fragment was amplified from an N-terminal HA-tagged DGK*ϵ* vector by 25 cycles using Pfu DNA polymerase (Stratagene) and "polished" with Taq DNA polymerase (Stratagene). The following primers were used: forward, 5′-GATCTGGAAGCGGAGAGGCGG-3′ [this primer contained a *Bgl*II site and corresponded to amino acids EAERR of human DGK*ϵ* (*9*)]; reverse, 5′-GTCGAC-TATTCAGTCGCCTTTATATC-3′ [this primer contained a *Sal*I site and corresponded to amino acids DIKATE of human DGK*ϵ* (*9*)]. An N-terminally truncated human DGK*ϵ* (DGKΔ*ϵ*) PCR fragment was amplified as described above for the full-length construct, except that the following primers were used: forward, 5′-AGATCTCCAGCGGTCGCGCC-3′ [this primer contained a *Bgl*II site and corresponded to amino acids LQRSR of human DGK*ϵ* (*9*)]; reverse, 5′-GTCGACTATTCAGTCGCCTTTATATC-3′ [this primer contained a *Sal*I site and corresponded to amino acids DIKATE of human DGK*ϵ* (*9*)]. The resulting PCR fragments were gel-purified and cloned into a TOPO-TA cloning vector (Invitrogen). The DNA fragments of interest were excised from the TOPO-TA vector using *Bgl*II and *Sal*I restriction enzymes and gel-purified. The fragments of interest were subcloned into the corresponding site of a p3XFLAG-CMV-7.1 mammalian vector (Sigma-Aldrich), which attaches a FLAG epitope at the N-terminus of the protein.

*Cell Culture and Transfection of DGK*ϵ *in COS-7 Cells.* COS-7 cells were maintained in Dulbecco's modified Eagle's medium (DMEM, GIBCO/Invitrogen) containing 10% fetal bovine serum (FBS, GIBCO/Invitrogen) at 37 °C in an atmosphere of 5% CO_2. The p3XFLAG constructs were transiently transfected into COS-7 cells using Lipofectamine 2000 according to the manufacturer's instructions (Invitrogen). Cells were transfected in parallel with the p3XFLAG-CMV-7.1 vector as a control. A schematic representation of the constructs used in this work is shown in Figure 1.

*Estimation of the Amounts of FLAG-Tagged Recombinant DGK*ϵ *Proteins.* Amounts of FLAG-tagged DGK*ϵ* proteins in the membrane fractions of DGK transfectants were estimated by immunoblotting with a mouse anti-FLAG peptide M2 primary antibody (Sigma-Aldrich). A 3XFLAG-tagged bacterial alkaline phosphatase (3XFLAG-BAP, Sigma-Aldrich) with a molecular mass of 49.9 kDa was used as a

standard in different lanes of the same blots. The 3XFLAG-BAP used as a standard is similar in size and contains an epitope similar to that of the FLAG-DGK constructs. Proteins in the membrane fractions were solubilized with 30 mM OG, separated by SDS−PAGE (7.5% gel), and then transferred onto Immobilon-P polyvinylidene fluoride (PVDF) membranes (Millipore). Blotting was performed according to the manufacturer's instructions (Amersham Biosciences, GE Healthcare), using mouse anti-FLAG antibody followed by anti-mouse IgG secondary antibody conjugated with horseradish peroxidase (HRP) (Pierce Biotechnology). Immune complexes were detected using an ECL solution detection system (Amersham Biosciences, GE Healthcare) and visualized using a Typhoon scanner (Amersham Biosciences, GE Healthcare). The DGKϵ and BAP protein bands were quantified by densitometric scanning of the digitized image (tif file) using Scion image (Scion Image Corp.). A standard curve was created by blotting on the membrane increasing amounts of the 3XFLAG-BAP protein. The amounts of recombinant DGKϵ proteins were estimated from the sigmoidal curve of 3XFLAG-BAP protein using the sigmoidal (Boltzman) fit of the data.

Enzyme Preparations for Kinetic Analysis. The transfected cells were harvested after 24−48 h in ice-cold cell lysis buffer [20 mM Tris-HCl (pH 7.5), 150 mM NaCl, 1 mM EDTA, and Protease Inhibitor Cocktail (1×) (Sigma-Aldrich)]. The cells were pelleted at low speed (6000*g*), and the pellets were kept at −70 °C until further use. Prior to the assay, cell pellets were resuspended in cell lysis buffer containing 30 mM OG, allowed to lyse for 10 min on ice, and then centrifuged at 100000*g* for 30 min at 20 °C. The supernatants were used in the assay of DGK activity. Full-length human DGKϵ was also prepared from cell pellets of Sf21 insect cells infected with baculovirus stocks containing DGKϵ cloned into BacPAK6 and carrying a C-terminal 6XHis epitope.

DGK Activity Assay in OG Micelles. The assay was adapted from the method described by Walsh et al. (*10*). For each assay, DAG stock solutions (DOG, SAG, or SLG, in a 1:1 $CHCl_3/CH_3OH$ mixture) together with any other lipid component used in the assay were dried under a stream of N_2 gas in a glass test tube and evaporated under vacuum for 2 h to remove any traces of the solvent. The lipid was hydrated with 50 μL of 4× assay buffer [300 mM OG, 200 mM MOPS (pH 7.2), 400 mM NaCl, 20 mM $MgCl_2$, and 4 mM EGTA], 20 μL of 100 mM $CaCl_2$, 20 μL of 10 mM DTT, and 10−20 μL of cell lysate from cells transfected either with one of the DGKϵ preparations or with an extract from mock-transfected cells. For the determination of enzyme activity from the floatation assay, 110 μL fractions were used after ultracentrifugation. In cases where the floatation assay was conducted at high salt concentrations, the NaCl component was removed from the assay buffer so that the assay conditions would be similar for fractions containing salt as well as those without excess salt. The final volume was 180 μL. The reaction was initiated by adding 20 μL of 5.0 mM [γ-^{32}P]ATP (50 μCi/mL). The final assay mixture contained 75 mM OG, 50 mM MOPS (pH 7.2), 100 mM NaCl, 5 mM $MgCl_2$, 1 mM EGTA, 10 mM $CaCl_2$, 1 mM DTT, the enzyme preparation, a range of substrate concentrations from 0.12 to 0.96 mM, 3.5 mM phospholipids (unless otherwise noted), and 0.5 mM ATP. The reaction was carried out for 10 min at 25 °C and was terminated by extraction of the lipid with the addition of 2 mL of a $CHCl_3/CH_3OH$ mixture (1:1, v/v) containing 0.25 mg/mL dihexadecyl phosphate. The organic phase was washed three times with 2 mL each of 1% $HClO_4$ and 0.1% H_3PO_4 in a H_2O/CH_3OH mixture (7:1, v/v). The volume of the final $CHCl_3$ phase was 0.80 mL. A 0.40 mL aliquot of the organic phase was dried at 50 °C for 2 h, and the incorporation of ^{32}P into PA was assessed by Cerenkov counting. Controls were run with the addition of mock-transfected cell lysates or without the addition of lipid substrates. In both cases, the counts remaining in the organic phase were only slightly above background. The DGK activity measured with mock-transfected cells was subtracted from the values obtained using cells overexpressing one of the DGKϵ constructs. The production of PA was linear with time over 10 min. The assays were conducted in triplicate, and the results are presented with errors showing the standard deviation of the mean for one particular experiment. Each experiment was independently repeated at least two times. The day-to-day variations using the same enzyme preparation and the same lipids were not much greater than those for an individual experiment.

Kinetic Analysis of the Micelle-Based Assay of DGK Activity. A kinetic analysis was performed on the two different DGKϵ full-length constructs and on the DGKΔϵ truncated construct for each of the lipid substrates. The Michaelis−Menten constants, V_{max} and K_m, were evaluated by a least-squares fit of a two-parameter hyperbolic plots [initial velocity (v_0) vs substrate concentration ([S])] as well as by using Hanes plots ([S]/v_0 vs [S]). Total protein content was determined with a Bio-Rad protein assay kit (Bio-Rad). The content of FLAG-tagged DGKϵ protein was determined as described below. Microcal Origin was used to analyze the two plots, and the corresponding errors in k_{cat} and K_m were obtained using the data analysis function.

Floatation Assay for Separation of Membrane-Bound Enzyme from Soluble Enzyme. Cells transfected with one of the forms of DGKϵ (80 μL) were thawed on ice, and 400 μL hypotonic lysis buffer [5 mM sodium phosphate and 250 mM sucrose (pH 7.2)] was added to cells. Cells were mechanically sheared with a bent-tip syringe and centrifuged at 3000*g* for 5 min to remove nuclei and unbroken cells. For the salt-containing samples, KCl was added to the extracted supernatant to give a final KCl concentration of 1.5 M and a total volume of 800 μL. Samples lacking salt were taken to an 800 μL volume with the addition of lysis buffer. Samples were incubated on ice for 30 min and then adjusted with a stock iodixanol solution (OptiPrep, Axis-Shield) to generate 2 mL of 30% (w/v) iodixanol samples. This mixture was loaded at the bottom of a 5 mL polyallomer ultracentrifuge tube and overlaid with 2 mL of a 25% iodixanol solution and 0.8 mL of a 5% iodixanol solution, sequentially. The gradient was centrifuged at 200000*g* for 3 h at 4 °C in an Optima MAX ultracentrifuge (Beckman Coulter) using a MLS-50 swinging-bucket rotor. After centrifugation, equal volume fractions (300 μL) were collected from top to bottom, and the presence of DGKϵ was assessed by enzymatic activity as well as Western blot analysis. These assays were performed as described below, except that for the activity assays of fractions having a high salt concentration, the salt concentration of the assay buffer

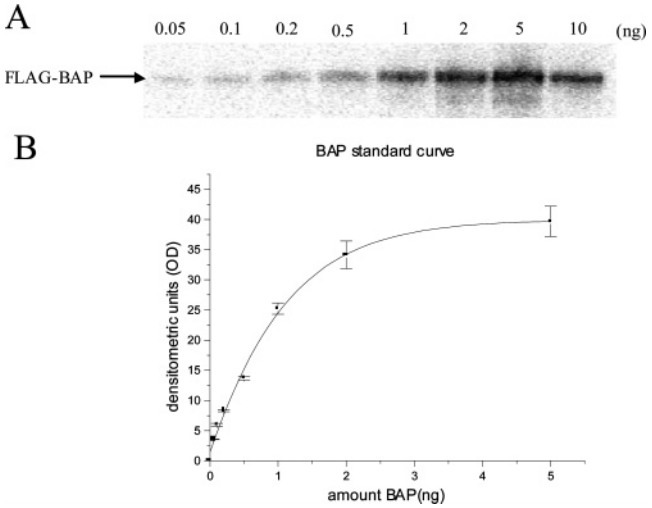

FIGURE 2: Calibration curve for the intensity of bands on Western blots. (A) Western blotting analysis of serial dilutions of 3XFLAG-tagged BAP protein. The intensity of the 49.9 kDa (BAP protein) bands increased with an increase in the content of 3XFLAG-tagged BAP protein. (B) Depiction of the relationship between the content of BAP protein and the band density. A sigmoidal (Boltzman) fit was obtained using Microcal Origin.

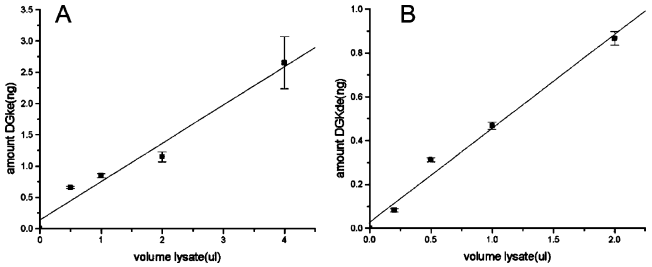

FIGURE 3: Relationship between the volume of the membrane protein lysate and the FLAG-DGKϵ protein content. (A) Curve depicting the relationship between the volume of the membrane protein lysate and the FLAG-DGKϵ protein content estimated from the BAP standard curve. (B) Curve depicting the relationship between the volume of the membrane protein lysate and the FLAG-DGK$\Delta\epsilon$ protein content estimated from the BAP standard curve. An estimation of the amount of each enzyme was calculated by using directly the sigmoidal (Boltzman) formula in the linear range of the curve.

was lowered so that the assay conditions would be identical with the fractions without excess salt.

PFO−PAGE Studies of Protein Oligomerization. To analyze the state of oligomerization of the enzyme in the lysates, PFO−PAGE on 7.5% Tris-HCl premade gels (Bio-Rad) was used. The protocol was adapted from Ramjeesingh et al. (*23*) and modified according to Yang et al. (*24*). The 2× sample buffer contained 100 mM Tris-HCl (pH 8.0), 0.2% NaPFO (Sigma-Aldrich), 20% glycerol, and 0.005% bromophenol blue, and the running buffer consisted of 25 mM Tris-HCl (pH 8.5), 192 mM glycine, and 0.1% NaPFO. The enzyme lysates were prepared as described above for the kinetic analysis. Prior to being loaded, cell pellets were suspended in cell lysis buffer containing 0.2% digitonin, allowed to lyse for 10 min on ice, and then centrifuged at 100000*g* for 30 min at 20 °C. The supernatants were loaded on the gel in serial dilutions using the above-mentioned lysis buffer and maintaining a constant detergent concentration. Amounts of FLAG-DGKϵ proteins and FLAG-DGK$\Delta\epsilon$ were estimated by immunoblotting with a mouse anti-FLAG peptide M2 primary antibody (Sigma-Aldrich).

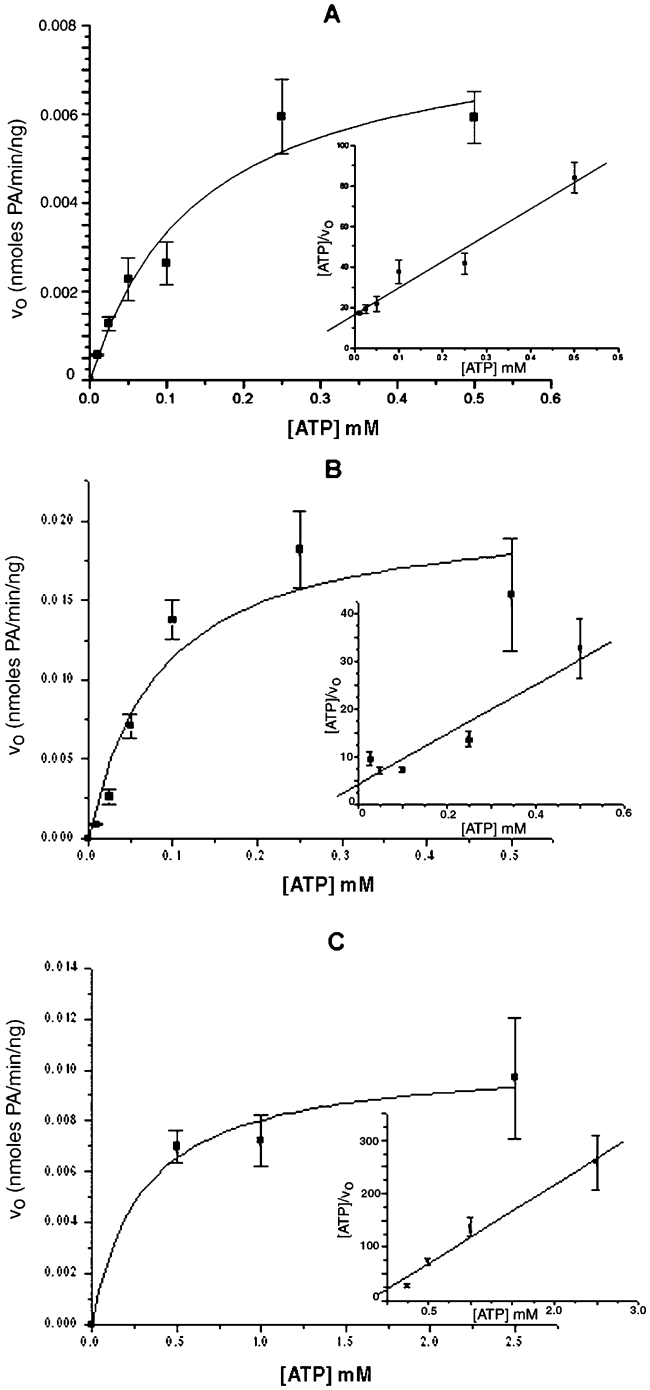

FIGURE 4: Dependence of the initial velocity (v_o) of DGK-catalyzed phosphorylation of SAG on ATP concentration. Two-parameter hyperbolic plot of initial velocity (v_o) vs substrate concentration. The inset shows a Hanes plot used to determine the Michaelis−Menten constants. The concentration of SAG was maintained at 1.5 mol %: (A) FLAG-DGKϵ, (B) FLAG-DGK$\Delta\epsilon$, and (C) DGKϵ-His. The data reported are an average of one experiment performed in triplicate. Error bars indicate the standard error of the mean.

RESULTS

Determination of the Concentration of FLAG-DGK. We measured an absolute concentration of DGK so we could compare the maximal rates from different enzyme preparations. This was done for FLAG-DGKϵ or FLAG-DGK$\Delta\epsilon$

Table 1: Apparent Michaelis−Menten Constants of DGKϵ with ATP as a Substrate[a]

isoform	substrate	K_m (mM)	k_{cat} (s^{-1})	k_{cat}/K_m (s^{-1} mM^{-1})
FLAG-DGKϵ	ATP	0.13 ± 0.03	8.2 ± 0.8	63
FLAG-DGKΔϵ	ATP	0.135 ± 0.06	23 ± 5	169
DGKϵ-His	ATP	0.2 ± 0.15	0.010 ± 0.0011[b]	0.05[b]

[a] Activity represents the average of at least two independent experiments performed triplicate. Errors represent the standard deviation among the two experiments under each condition. [b] The values of k_{cat} for DGKϵ-His are in nanomoles of PA per minute since the amount of protein in the lysates was not determined.

in extracts from COS-7 cells using Western blotting with an anti-FLAG antibody. The correspondence between the intensity of the band in Western blots and the amount of protein was determined by comparing with a standard of 3X-FLAG-tagged BAP protein (Figure 2). For quantification of DGK, we used only bands with an intensity lower than 25 units. The standard curves for either FLAG-DGKϵ or FLAG-DGKΔϵ exhibited good linearity with regression coefficients of 0.97 and 0.99, respectively (Figure 3). Attempts to do a similar analysis with DGKϵ-His using an anti-His tag antibody (Amersham Biosciences) or an anti-DGKϵ antibody (Santa Cruz Biotech) did not yield a reliable standard curve for quantification. The enzyme activity for this construct is presented only in relative terms for different substrates.

Kinetic Analysis of ATP as a Substrate. In the process of phosphorylation of DAG, DGKϵ utilizes two substrates, a water-soluble substrate, ATP, and a water-insoluble substrate, DAG. Each of these substrates binds to the enzyme at different sites. There are also different consequences for the kinetics because one of the substrates is water-soluble while the other is not. The binding of ATP to the enzyme is assessed by its concentration in the total volume of the solution, which is common for other enzyme catalysis. To determine the apparent dissociation constant (K_m) for dissociation of ATP from the enzyme, we varied the ATP concentration at a constant high concentration of SAG (1.5 mol %) and examined the effect on the catalytic activity. We show the dependence of the initial velocity on the concentration of ATP for FLAG-DGKϵ, FLAG-DGKΔϵ, and DGKϵ-His (Figure 4). The values of $K_{m(ATP)}$ and k_{cat} are summarized in Table 1. There is no significant difference in $K_{m(ATP)}$ for any of the three forms of DGKϵ that were used. The value of k_{cat} is significantly larger for FLAG-DGKΔϵ than for FLAG-DGKϵ. In the case of DGKϵ-His, the value of k_{cat} is relative since the concentration of this construct could not accurately be determined.

Kinetic Analysis of DAG as a Substrate. The kinetic assays were conducted in a DAG/detergent/phospholipid mixed micellar system using a high concentration of ATP (0.5 mM). The presence of the phospholipid was required since at higher substrate concentrations aggregation was noticed in its absence. The concentration of DAG substrate is expressed as its mole fraction in the lipid/detergent mixture. The binding of the lipid substrate to the catalytic site is assessed not by its bulk concentration but by its concentration within the water-insoluble phase of micelles (*25*). The initial rate of the enzyme-catalyzed reaction was determined as a function of the concentration of SAG in the micellar phase (Figure 5). A similar analysis was carried out for SLG and DOG. The kinetic properties of different forms of DGKϵ phosphorylating three different lipid substrates are summarized in Table 2. For all three of the constructs, there is specificity for DAG species with polyunsaturated acyl chains, with SAG being a better substrate than SLG. In general, the higher activity seen with SAG is a result of contributions from both a lower value of K_m and a higher value of k_{cat}. As with ATP, the k_{cat} for FLAG-DGKΔϵ is greater than for FLAG-DGKϵ. However, the values of k_{cat} are several-fold lower for the DAGs than for ATP, although they should be the same. We ascribe the difference to the fact that the DAGs are an interfacial substrate and it is more difficult to reach a maximal limiting concentration without altering the properties of the micelle. The ATP substrate is of course water-soluble and does not suffer from the complications of interfacial catalysis.

Extractability of DGKϵ and DGKΔϵ from the COS-7 Cell Membranes. We established, using sucrose density gradient centrifugation (*26*), that both DGKϵ and DGKΔϵ were found in the membrane fraction together with the plasma membrane marker, 5′-nucleotidase (*27*). Density gradient ultracentrifugation using iodixanol (*28*) allowed for the separation of membrane-bound DGK from soluble forms of the enzyme by floatation of the membranes. The method gives a clear separation between the fractions containing low-density lipid-containing membrane particles concentrated in fractions 3−5 and the fractions containing the soluble form of the enzyme found in fractions 10−15 (Figure 6). The ratio of the total amount of enzyme in each of these two fractions is summarized in Table 3, based on enzyme activity measurements. The presence of the enzyme in the fractions having DGK activity was confirmed by Western blotting. However, in cases where high salt concentrations were used to extract the enzyme, the proteins migrated aberrantly on the gels. We therefore based the membrane partitioning results on the activity measurements, since the presence of salt hindered the Western blot analysis. We can conclude that the FLAG tag does not have a major effect on membrane partitioning since full-length DGKϵ and FLAG-DGKϵ behave similarly in the presence or absence of salt at neutral pH. However, the hydrophobic segment does have a significant effect on membrane partitioning. This is most clearly demonstrated in the absence of salt where much more FLAG-DGKΔϵ dissociates from the membrane than FLAG-DGKϵ.

Oligomerization in PFO−PAGE. Assessment of the quaternary structure of membrane proteins by PAGE has been problematic due to the relatively poor solubility of membrane proteins in nondissociative detergents. In SDS−PAGE, all forms of DGKϵ used in this work run as a monomer. A novel method for evaluating the oligomeric structure of membrane proteins uses the perfluorooctanoic acid (PFO) detergent, which is less denaturing than SDS and allows assessment of multimeric protein complexes in the gel (*23*). This was done for both the full-length FLAG-DGKϵ

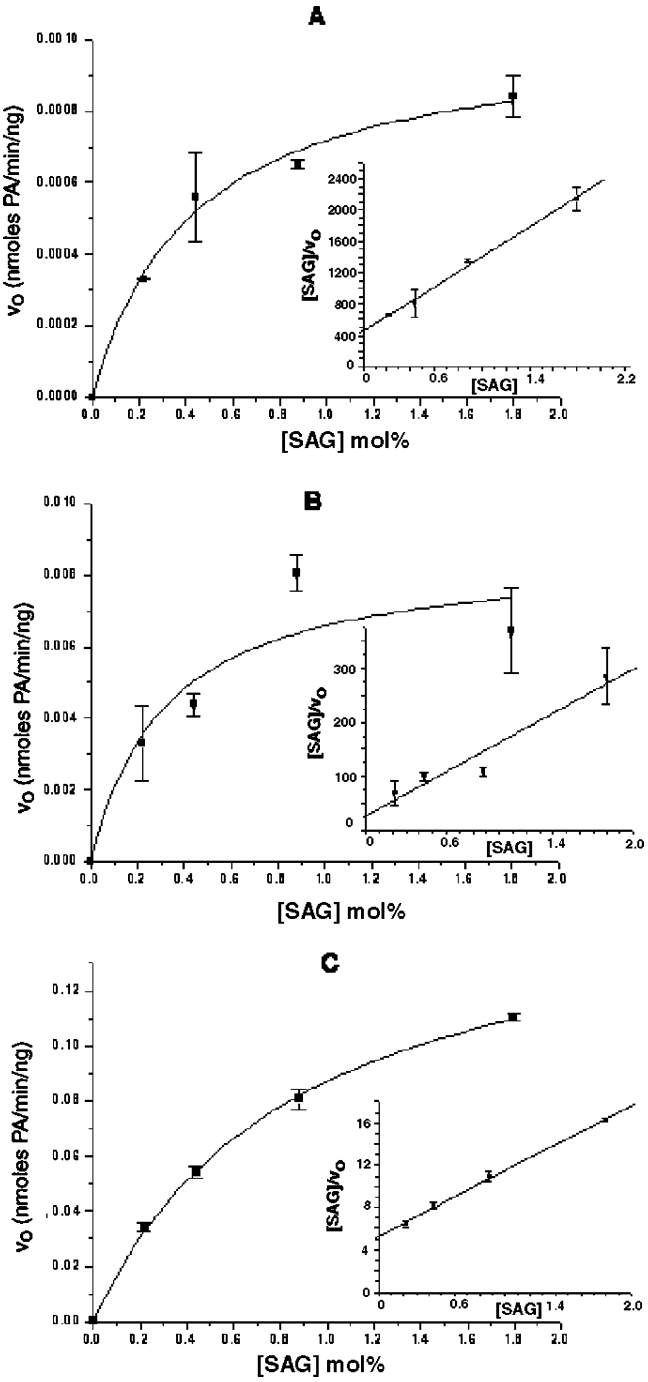

FIGURE 5: Dependence of the initial velocity (v_o) of DGK-catalyzed phosphorylation of SAG. Two-parameter hyperbolic plot of initial velocity (v_o) vs substrate concentration. The ATP concentration was kept constant at 0.5 mM. The inset shows a Hanes plot used to determine the Michaelis−Menten constants: (A) FLAG-DGKϵ, (B) FLAG-DGK$\Delta\epsilon$, and (C) DGKϵ-His. The data reported are an average of two experiments performed in triplicate. Error bars indicate the standard error of the mean.

and the truncated FLAG-DGK$\Delta\epsilon$ as a function of protein concentration. The monomer:dimer ratio increases as the dilution of the protein increases. The result is more noticeable for the FLAG-DGK$\Delta\epsilon$ construct. Also, the monomer:dimer ratio is higher for the FLAG-DGK$\Delta\epsilon$ construct than for the FLAG-DGKϵ construct (Figure 7). Since the higher-molecular weight band is exactly twice the lower-molecular weight band, the simplest explanation is that this is a monomer−dimer equilibrium. However, we cannot rigorously exclude the possibility that DGKϵ is binding to another protein with a similar molecular weight.

Table 2: Apparent Michaelis−Menten Constants of DGKϵ with DAGs as Substrates[a]

isoform[b]	substrate	K_m (mol %)	k_{cat} (s^{-1})	k_{cat}/K_m (s^{-1} mol $\%^{-1}$)
FLAG-DGKϵ	SAG	0.54 ± 0.13	1.7 ± 0.9	3.1
FLAG-DGKϵ	SLG	0.65 ± 0.08	1.23 ± 0.02	1.9
FLAG-DGKϵ	DOG	2.5 ± 2.2	1.2 ± 0.2	0.48
FLAG-DGK$\Delta\epsilon$	SAG	0.97 ± 0.11	5.7 ± 0.38[c]	5.9
FLAG-DGK$\Delta\epsilon$	SLG	0.8 ± 0.1	2.8 ± 0.99[c]	3.5
FLAG-DGK$\Delta\epsilon$	DOG	1.2 ± 0.3	2.43 ± 0.09	2.0
DGKϵ-His	SAG	0.85 ± 0.04	0.162 ± 0.005[d]	0.191[d]
DGKϵ-His	SLG	0.51 ± 0.04	0.087 ± 0.011[d,e]	0.171[d]
DGKϵ-His	DOG	2.7 ± 0.2	0.032 ± 0.001[d]	0.0119[d]

[a] Activity represents the average of at least two independent experiments performed in triplicate. Errors represent the standard deviation between the two experiments under each condition. [b] Nature of the epitope tag included to distinguish between the two forms of DGKϵ that were used. [c] The k_{cat} values were calculated using direct linear plots and Hanes plots. [d] Values of k_{cat} are relative values since the amount of enzyme in the cell preparations is not known. [e] The k_{cat} value for SLG is calculated relative to the k_{cat} for SAG at the same enzyme concentration and at the maximal substrate concentration.

DISCUSSION

DGKϵ is unique among known mammalian DGK isoforms in having a hydrophobic segment that is predicted to be a transmembrane helix by several algorithms, including IMPALA (*29*), TM finder (*30*), and DAS (*31*). This isoform is also unique in exhibiting specificity for DAG containing arachidonoyl acyl chains. Our results demonstrate that even complete removal of this putative transmembrane domain did not have any effect on substrate specificity (Table 2). Furthermore, the truncation of the enzyme actually caused an increase in the catalytic rate constant. However, this effect is relatively modest compared with the increase in the catalytic rate observed with DGKα upon N-terminal truncation. Removal of the EF-hands at the N-terminus of DGKα results in a mutant form whose activity is completely independent of Ca^{2+} (*32*, *33*). Nevertheless, there may be a relationship between the two cases in that loosening the structure of the DGK removes an inhibitory domain from the active site. Thus, the hydrophobic N-terminal segment of DGKϵ does not contribute to either enzymatic activity or substrate specificity. We therefore explored how this segment affected interactions of the protein with membranes.

The difference between a peripheral and integral membrane protein is based on a phenomenological definition. Integral membrane proteins can be extracted from a membrane only by disrupting the membrane structure. Although DGKϵ has a hydrophobic segment that is predicted to be inserted into the membrane, the protein does not behave like an integral membrane protein in that it can be extracted with high concentrations of KCl (*10*). In the absence of excess salt, we find that essentially all of the full-length DGKϵ at neutral pH is found in a low-density fraction, indicating that it is strongly partitioned into the membrane (Table 3 and Figure 6). This finding is independent of whether there is a FLAG tag. Nevertheless, a significant fraction of this full-length DGKϵ can be extracted from the membrane with 1.5 M KCl, indicating that the protein does not behave as an integral membrane protein and can be extracted from the

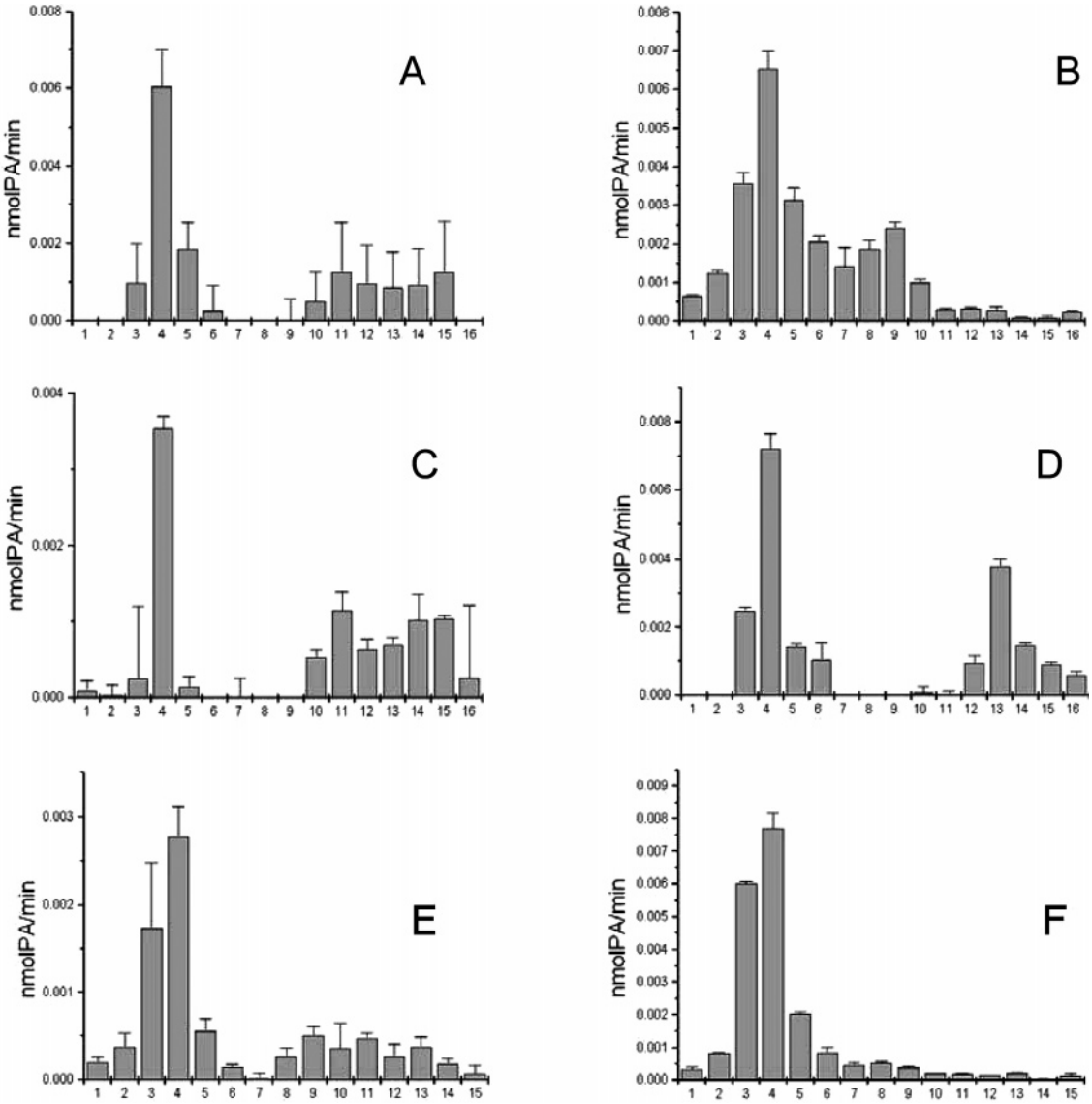

FIGURE 6: Enzyme activity analysis of fractions collected by floatation assay with or without prior treatment of cells with salt at neutral pH. Bar graphs reflect the DGK enzyme activity vs collected fraction number. Fractions 3−6 were classified as membrane-associated, and fractions 10−15 were considered to be cytoplasmic or soluble fractions. Cells were suspended either in 5 mM sodium phosphate and 250 mM sucrose (pH 7.2) (without salt) or in this buffer with 1.5 M KCl (with salt): (A) FLAG-DGKϵ with salt, (B) FLAG-DGKϵ without salt, (C) FLAG-DGKΔϵ with salt, (D) FLAG-DGKΔϵ without salt, (E) DGKϵ with salt, and (F) DGKϵ without salt.

Table 3: Partitioning of DGKϵ between Soluble and Membrane Fractions Determined by the Floatation Assay

construct	condition	membrane/soluble
DGKϵ (no epitope tag)	no salt addition	>10
DGKϵ (no epitope tag)	1.5 M KCl	1.09
FLAG-DGKϵ	no salt addition	>10
FLAG-DGKϵ	1.5 M KCl	1.12
FLAG-DGKΔϵ	no salt addition	0.95
FLAG-DGKΔϵ	1.5 M KCl	0.73

membrane with high salt concentrations. We compared this behavior with that of a DGKϵ construct lacking the 40 N-terminal amino acid residues. It is clear that this region of the protein contributes significantly to the membrane partitioning of the protein (Table 3 and Figure 6). Nevertheless, even without this hydrophobic segment and in the presence of 1.5 M KCl, a fraction of the protein remains membrane-associated, indicating that other regions of the molecule contribute to membrane binding. In this context, it should be pointed out that transmembrane helical prediction algorithms also identify the region between residues 450 and 460 as being a transmembrane, but this segment is significantly less hydrophobic than the region of residues 20−40. In addition, all the DGK isoforms act on a lipid substrate, DAG, that is integrated into the membrane. Therefore, to be active, these proteins must have the capability of partitioning to a membrane. This also holds true for DGK isoforms apart from DGKϵ that do not contain a putative transmembrane segment.

Using a model peptide corresponding to the putative transmembrane domain of DGKϵ, we showed both by SDS−PAGE and by FRET analysis that the peptide had a strong tendency to oligomerize (manuscript in preparation). This finding was in accord with molecular modeling studies that predicted the formation of stable transmembrane dimers. However, in the context of the full-length protein, self-association of the protein could only be demonstrated at low concentrations of PFO. Under these conditions, there is some dimer formed; this dimer formation is dependent on the

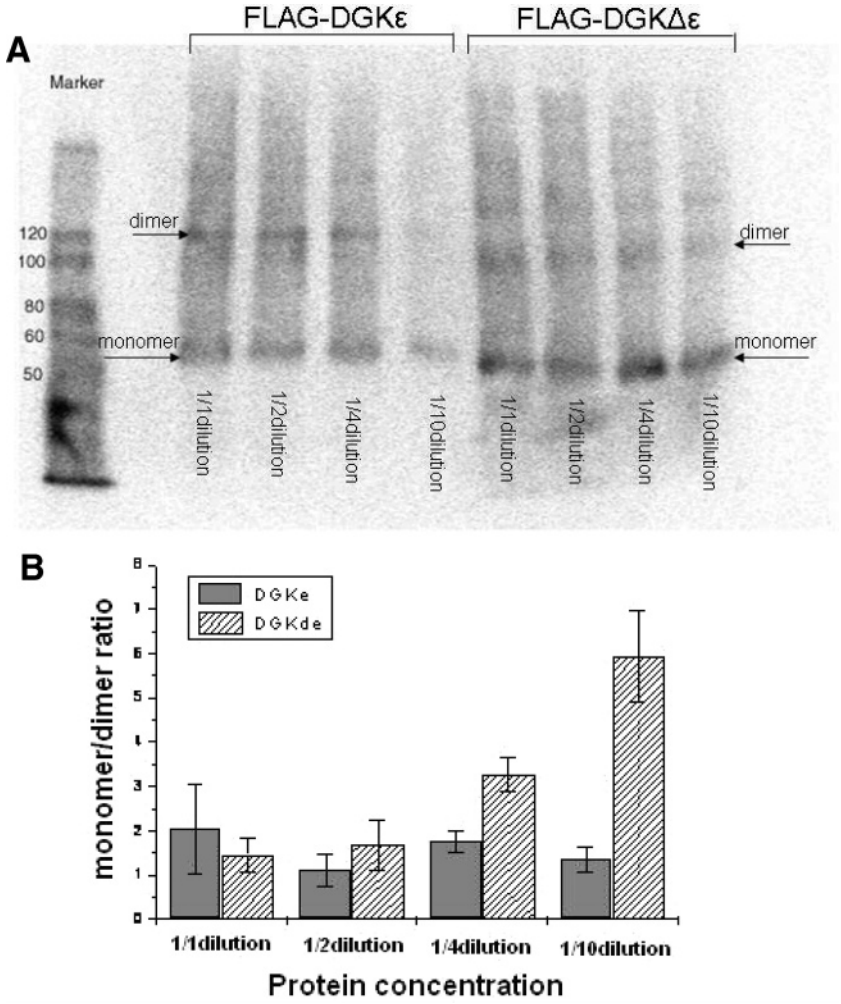

FIGURE 7: (A) Oligomerization of FLAG-DGKϵ and FLAG-DGK$\Delta\epsilon$ via PFO−PAGE. The enzyme lysates were prepared as noted in Experimental Procedures. Four bands were loaded for each protein. The dilution of the protein was conducted in the lysis buffer maintaining a constant detergent concentration. Amounts of FLAG-DGKϵ proteins and FLAG-DGK$\Delta\epsilon$ were estimated by immunoblotting with a mouse anti-FLAG peptide M2 primary antibody (Sigma-Aldrich). The presence of monomer or dimer was monitored by the presence of a band corresponding to 65 or 130 kDa, respectively. (B) Ratio between the band intensity for FLAG-DGKϵ and the band intensity for FLAG-DGK$\Delta\epsilon$ from PFO gels. The intensity of the bands from Western blots (Figure 5A) was determined with Scion Image. The mean intensity of five readings for each of the bands was calculated, and the background intensity was subtracted. The ratio was calculated by dividing the average density of the monomer band by the average density of the dimer band.

presence of the N-terminal hydrophobic segment, and the extent of formation increases with protein concentration (Figure 7). However, the protein oligomer is less stable than that observed with the peptide and is not seen in SDS or even at 0.5% PFO, but only at the lower PFO concentration of 0.1%. In addition, we attempted to detect oligomerization using chemical cross-linking with disuccinimidyl suberate. This method showed a weak band corresponding to a cross-linked tetramer. However, this higher-molecular weight band appeared both with FLAG-DGKϵ and with FLAG-DGK$\Delta\epsilon$ (not shown). Finally, we attempted co-immunoprecipitation of a mixture of N-terminally FLAG-tagged or HA-tagged constructs. With proteins extracted into 30 mM OG, the anti-FLAG antibody brought down only the FLAG-tagged construct (not shown). In summary, there is some evidence for oligomerization of DGKϵ that is transiently stable. The hydrophobic segment contributes to this process as seen with the results from the PFO gels (Figure 7), but other regions of the molecule may also contribute.

Although DGKϵ is unique among mammalian DGK isoforms in having a putative transmembrane segment, this segment is not responsible for the other unique property of this isoform of being specific for arachidonoyl-containing substrates. We suggest that the hydrophobic segment has a different role in modulating the biological properties of this isoform. The amino-terminal segment of DGKϵ contributes to the incorporation of the protein into a membrane as well as facilitating oligomerization of the protein. In the context of a cell membrane, the role may be more specific in partitioning the protein into a region of the membrane by interacting with hydrophobic regions of a lipid domain or of particular membrane proteins. It is suggestive that this domain causes the enrichment of DGKϵ in regions of the membrane in which DAG will be liberated by the action of phospholipase C on PtdIns(4,5)P2, thus functionally linking the high arachidonoyl content of this phospholipid with the substrate specificity of DGKϵ.

REFERENCES

1. Topham, M. K. (2006) Signaling roles of diacylglycerol kinases, *J. Cell. Biochem. 97*, 474−484.
2. Catt, K. J., and Balla, T. (1989) Phosphoinositide metabolism and hormone action, *Annu. Rev. Med. 40*, 487−509.

3. Brose, N., and Rosenmund, C. (2002) Move over protein kinase C, you've got company: Alternative cellular effectors of diacylglycerol and phorbol esters, *J. Cell Sci. 115*, 4399−4411.
4. Bazan, N. G. (2005) Lipid signaling in neural plasticity, brain repair, and neuroprotection, *Mol. Neurobiol. 32*, 89−103.
5. Musto, A., and Bazan, N. G. (2006) Diacylglycerol kinase ϵ modulates rapid kindling epileptogenesis, *Epilepsia 47*, 267−276.
6. Rodriguez de Turco, E. B., Tang, W., Topham, M. K., Sakane, F., Marcheselli, V. L., Chen, C., Taketomi, A., Prescott, S. M., and Bazan, N. G. (2001) Diacylglycerol kinase ϵ regulates seizure susceptibility and long-term potentiation through arachidonoyl-inositol lipid signaling, *Proc. Natl. Acad. Sci. U.S.A. 98*, 4740−4745.
7. Gaudette, D. C., Aukema, H. M., Jolly, C. A., Chapkin, R. S., and Holub, B. J. (1993) Mass and fatty acid composition of the 3-phosphorylated phosphatidylinositol bisphosphate isomer in stimulated human platelets, *J. Biol. Chem. 268*, 13773−13776.
8. Mauco, G., Dangelmaier, C. A., and Smith, J. B. (1984) Inositol lipids, phosphatidate and diacylglycerol share stearoylarachidonoylglycerol as a common backbone in thrombin-stimulated human platelets, *Biochem. J. 224*, 933−940.
9. Tang, W., Bunting, M., Zimmerman, G. A., McIntyre, T. M., and Prescott, S. M. (1996) Molecular cloning of a novel human diacylglycerol kinase highly selective for arachidonate-containing substrates, *J. Biol. Chem. 271*, 10237−10241.
10. Walsh, J. P., Suen, R., Lemaitre, R. N., and Glomset, J. A. (1994) Arachidonoyl-diacylglycerol kinase from bovine testis. Purification and properties, *J. Biol. Chem. 269*, 21155−21164.
11. Pettitt, T. R., and Wakelam, M. J. (1999) Diacylglycerol kinase ϵ, but not ζ, selectively removes polyunsaturated diacylglycerol, inducing altered protein kinase C distribution in vivo, *J. Biol. Chem. 274*, 36181−36186.
12. Topham, M. K., and Prescott, S. M. (2001) Diacylglycerol kinase ζ regulates Ras activation by a novel mechanism, *J. Cell Biol. 152*, 1135−1143.
13. Luo, B., Regier, D. S., Prescott, S. M., and Topham, M. K. (2004) Diacylglycerol kinases, *Cell. Signalling 16*, 983−989.
14. Avila-Flores, A., Santos, T., Rincon, E., and Merida, I. (2005) Modulation of the mammalian target of rapamycin pathway by diacylglycerol kinase-produced phosphatidic acid, *J. Biol. Chem. 280*, 10091−10099.
15. Yang, C., and Kazanietz, M. G. (2003) Divergence and complexities in DAG signaling: Looking beyond PKC, *Trends Pharmacol. Sci. 24*, 602−608.
16. Imai, S., Kai, M., Yasuda, S., Kanoh, H., and Sakane, F. (2005) Identification and characterization of a novel human type II diacylglycerol kinase, DGKκ, *J. Biol. Chem. 280*, 39870−39881.
17. Van Blitterswijk, W. J., and Houssa, B. (2000) Properties and functions of diacylglycerol kinases, *Cell. Signalling 12*, 595−605.
18. Sakane, F., and Kanoh, H. (1997) Molecules in focus: Diacylglycerol kinase, *Int. J. Biochem. Cell Biol. 29*, 1139−1143.
19. Kanoh, H., Yamada, K., and Sakane, F. (2002) Diacylglycerol kinases: Emerging downstream regulators in cell signaling systems, *J. Biochem. 131*, 629−633.
20. Topham, M. K., and Prescott, S. M. (1999) Mammalian diacylglycerol kinases, a family of lipid kinases with signaling functions, *J. Biol. Chem. 274*, 11447−11450.
21. Topham, M. K., and Prescott, S. M. (2002) Diacylglycerol kinases: Regulation and signaling roles, *Thromb. Haemostasis 88*, 912−918.
22. Thirugnanam, S., Topham, M. K., and Epand, R. M. (2001) Physiological implications of the contrasting modulation of the activities of the ϵ and ζ isoforms of diacylglycerol kinase, *Biochemistry 40*, 10607−10613.
23. Ramjeesingh, M., Huan, L. J., Garami, E., and Bear, C. E. (1999) Novel method for evaluation of the oligomeric structure of membrane proteins, *Biochem. J. 342* (Part 1), 119−123.
24. Yang, Z. G., Liu, Y., Mao, L. Y., Zhang, J. T., and Zou, Y. (2002) Dimerization of human XPA and formation of XPA2-RPA protein complex, *Biochemistry 41*, 13012−13020.
25. Carman, G. M., Deems, R. A., and Dennis, E. A. (1995) Lipid signaling enzymes and surface dilution kinetics, *J. Biol. Chem. 270*, 18711−18714.
26. Liscum, L., Ruggiero, R. M., and Faust, J. R. (1989) The intracellular transport of low density lipoprotein-derived cholesterol is defective in Niemann-Pick type C fibroblasts, *J. Cell Biol. 108*, 1625−1636.
27. Dicu, A. O. (2006) Investigation of diacylglycerol kinase ϵ, M.Sc. Thesis, McMaster University, Hamilton, ON, pp 1−108.
28. Graham, J., Ford, T., and Rickwood, D. (1994) The preparation of subcellular organelles from mouse liver in self-generated gradients of iodixanol, *Anal. Biochem. 220*, 367−373.
29. Ducarme, P., Rahman, M., and Brasseur, R. (1998) IMPALA: A simple restraint field to simulate the biological membrane in molecular structure studies, *Proteins 30*, 357−371.
30. Deber, C. M., Wang, C., Liu, L. P., Prior, A. S., Agrawal, S., Muskat, B. L., and Cuticchia, A. J. (2001) TM Finder: A prediction program for transmembrane protein segments using a combination of hydrophobicity and nonpolar phase helicity scales, *Protein Sci. 10*, 212−219.
31. Cserzo, M., Wallin, E., Simon, I., von Heijne, G., and Elofsson, A. (1997) Prediction of transmembrane α-helices in prokaryotic membrane proteins: The dense alignment surface method, *Protein Eng. 10*, 673−676.
32. Abe, T., Lu, X., Jiang, Y., Boccone, C. E., Qian, S., Vattem, K. M., Wek, R. C., and Walsh, J. P. (2003) Site-directed mutagenesis of the active site of diacylglycerol kinase α: Calcium and phosphatidylserine stimulate enzyme activity via distinct mechanisms, *Biochem. J. 375*, 673−680.
33. Jiang, Y., Qian, W., Hawes, J. W., and Walsh, J. P. (2000) A domain with homology to neuronal calcium sensors is required for calcium-dependent activation of diacylglycerol kinase α, *J. Biol. Chem. 275*, 34092−34099.

BI6024726